Pharm Res (2012) 29:448–459
DOI 10.1007/s11095-011-0555-x

RESEARCH PAPER

Comparative Investigations on *In Vitro* Serum Stability of Polymeric Micelle Formulations

Tobias Miller • Reinhard Rachel • Ahmed Besheer • Senta Uezguen • Markus Weigandt • Achim Goepferich

Received: 23 May 2011 / Accepted: 2 August 2011 / Published online: 31 August 2011

ABSTRACT

Purpose Stability of polymeric micelles upon injection is essential for a drug delivery system but is not fully understood. We optimized an analytical test allowing quantification of micellar stability in biofluids and applied it to a variety of block copolymer micelles with different hydrophobic block architechtures.

Methods Polymeric micelles were prepared from four different polymers and investigated via encapsulation of two fluorescent dyes. Samples were incubated in human serum; changes in Foerster Resonance Energy Transfer (FRET) were recorded as a function of time. This fluorescence-based approach was supported semi-quantitatively by results from Asymmetrical Flow Field-Flow-Fractionation (AF4).

Results After incubation experiments, micellar stability was determined by calculation of two stability-indicating parameters: residual micellar fractions (RMFs) and *in vitro* serum half-lives. Both parameters showed that PEG-PVPy micelles rapidly destabilized after 3 h (RMF < 45%), whereas PEG-PLA, PEG-PLGA and PEG-PCL micelles were far more stable (RMFs 65 to 98%).

Conclusion This FRET-based assay is a valuable tool in evaluating and screening serum stability of polymeric micelles and revealed low serum stability of PEG-PVPy micelles compared to polyester-based micelles.

KEY WORDS field flow fractionation · foerster resonance energy transfer · polymeric micelles · serum stability · transmission electron microscopy

INTRODUCTION

During the past 20 years of drug research, the number of newly developed poorly soluble compounds has steadily increased. Estimations suggest that 40% of new chemical entities have an aqueous solubility problem that consequently leads to insufficient bioavailability and undesired low therapeutic effects (1).

Varying approaches have been investigated to conquer solubility problems by formulation processes. Several highly fascinating and yet challenging options can be found in the field of nanosized carrier systems. For example, polymeric micelles seem to be highly promising for overcoming the problem outlined above. This drug delivery system can be formed from amphiphilic block copolymers leading to spherical nanosized particles with a hydrophobic core surrounded by a hydrophilic shell. In the core, these particles can host hydrophobic drugs, whereas the shell-forming corona confers the drug delivery system stealth properties and, as a result, a less distinct recognition by the

T. Miller • A. Besheer • S. Uezguen • M. Weigandt
Exploratory Pharmaceutical Development, Merck KGaA
Frankfurter Straße 250
64293 Darmstadt, Germany

R. Rachel
Center for Electron Microscopy at the Institute for Anatomy
University of Regensburg
Universitätsstrasse 31
93040 Regensburg, Germany

T. Miller • A. Goepferich (✉)
Department of Pharmaceutical Technology, University of Regensburg
Universitätsstrasse 31
93040 Regensburg, Germany
e-mail: achim.goepferich@chemie.uni-regensburg.de

A. Besheer
Dept. of Pharmacy, Pharmaceutical Technology & Biopharmaceutics
Ludwig Maximilians University
81377 Munich, Germany

mononuclear phagocyte system (MPS) (2–5). Such pegylated nanoparticles could achieve long blood circulation times and, thus, can target tumors passively by the enhanced permeation and retention (EPR) effect (6) or actively using appropriate ligands (7–9). Currently, the most advanced micellar formulations encapsulating the hydrophobic drug Paclitaxel have already entered the market in India (Nanoxel®) and Korea (Genexol-PM®) (10).

Generally, when working with polymeric micelles, there are two methods to encapsulate drugs: physical entrapment in the hydrophobic core or chemically linking the drug to the polymer chain by a covalent bond. Both approaches have their advantages. The physical entrapment of the drug is generally easier to prepare and leads to higher loading rates, while the chemical coupling confers the polymer-drug adduct a higher stability upon injection (11).

Consequently, the fate of micelles with physically incorporated drugs after intravenous application is a very critical issue. Generally, micelles are in dynamic equilibrium and tend to disassemble upon dilution below their critical aggregation concentration. Contrary to the low molar mass surfactants, polymeric micelles are known to be kinetically stable, taking hours to disassemble. However, while circulating in the blood, the polymeric micelles can lose their drug payload due to multiple reasons, including: 1) diffusion of the drug due to the small diffusion length; 2) partitioning between the hydrophobic micellar core and the surrounding aqueous phase, as well as binding to serum proteins or lipid membranes; and 3) eventual disassembly of the micelles themselves due to the strong dilution below their critical aggregation concentration (CAC) (12). Such premature release can lead to undesired pharmacokinetics and/or severe side effects, including the triggering of immunotoxicological cascades (13).

Considering these problems, the aim of this study was to investigate the *in vitro* stability of polymeric micelles made of different block copolymers, namely PEG-PVPy (PEG-poly-4-(vinylpyridine)), PEG-PLA (PEG-poly (lactide)), PEG-PLGA (PEG-poly(lactide-co-glycolide)) and PEG-PCL (PEG-poly(ε-caprolactone)) based on an analytical test we have adapted from the literature (14,15) and then further improved. Additionally, the stability of these polymeric micelles were benchmarked against those of Tween 80®, which was selected as an ideal reference non-ionic surfactant due to the presence of already published studies in humans.

For our *in vitro* studies, the two fluorescent dyes 1, 1′-Dioctadecyl-3,3,3′,3′-tetramethylindocarbocyanine perchlorate (DiI) and 3,3′-Dioctadecyloxacarbocyanine perchlorate (DiO) were incorporated into micelles as a model for physically entrapped drugs. When both dyes are in close proximity, Foerster Resonance Energy Transfer (FRET) can be measured and, hence, be used as a marker for micellar integrity. To study the serum stability of PEG-PVPy micelles *in vitro* and to compare the results with previously investigated block copolymers by other groups, we have refined the FRET-based technique. In contrast to the existing studies of Chen *et al.* (15) that calculate a FRET ratio from fluorescence maximum peak height, we integrated the recorded fluorescence spectra. This minimizes effects caused by changes in Stokes shifts from fluorescence dyes due to hydrophobic interactions of dye and polymer, as shown previously for poly(4-vinylpyridine) by Kamat and Fox (16). In addition, we were able to achieve complete dye release after incubation from the still intact polymeric micelles by addition of 7.5% *v/v* TritonX-100 at 37°C. This non-ionic surfactant leads to the dissolution of polymeric micelles, as indicated by Cerritelli *et al.* for PEG-PPS micelles (17). The resulting FRET ratio after complete dye release and the initial ratio enable the calculation of two parameters reflecting the stability of micelles: the *in vitro* serum half-life and residual micellar fraction (RMF).

Some of the investigated materials (PEG-PLA, PEG-PLGA and PEG-PCL) are well-known block copolymers, and their micelles have been thoroughly investigated. Gref *et al.* studied the influence of PEG chain length, PEG surface density, and different types of hydrophobic cores (PLA, PLGA and PCL) on plasma protein absorption by two-dimensional electrophoresis. This group identified a pattern of different proteins adsorbing onto the nanoparticulate surfaces (18). The different micellar hydrophobic cores showed qualitatively similar adsorption patterns with varying degrees in quantity of each serum protein fraction. Additionally, PEG-PCL micelles were investigated by Aliabadi *et al.* concerning their *in vivo* pharmacokinetic behavior (19). This was correlated with an *in vitro* serum stability experiment in which micelles were dialyzed against serum proteins to determine the non-encapsulated drug fraction. The authors correlated high micellar *in vivo* stability with the occurrence of low unbound drug fraction.

As previously mentioned, Chen *et al.* (14) have already shown by using a FRET-based method for PEG-PDLLA micelles that the stability depends on the influence of varying serum proteins and red blood cells. This group calculated FRET ratios from the emission maxima in the fluorescence spectra and discussed the impact of varying serum proteins and red blood cells on stability qualitatively. Furthermore, this technique has been applied to trace cellular uptake of intact micelles which physically encapsulate the dyes by confocal laser microscopy (15). Savic *et al.* conjugated a fluoresceine derivative covalently to PEG-PCL micelles and performed cellular uptake studies. They were able to distinguish between intact micelles and single

polymer chains (20). These existing methods, however, lack the possibility to quantify the micelles in human serum and to directly compare between formulations composed of block copolymers with different architectures.

MATERIALS AND METHODS

Materials

The following block copolymers were purchased from Polymer Source Inc, Montreal, Canada: mPEG-PLLA [5-b-4.7], mPEG-PDLLA [5-b-23], mPEG-PCL [5-b-32.5], mPEG-Poly-(4-vinylpyridine) [mPEG-PVPy] [2-b-5.5], mPEG-PVPy [2-b-10] and mPEG-PVPy [5-b-20]. PEG-PLGA [5-b-28] (Resomer RGP d 50155) was obtained from Boehringer Ingelheim, Ingelheim, Germany. Pyrene, tetrahydrofurane (THF) and acetone were delivered by VWR, Darmstadt, Germany. Tween 80®, human serum from male (blood group AB), and fluorescent dyes DiI and DiO were obtained from Sigma Aldrich, Rossdorf, Germany. SpectraPor dialysis tubing with MWCO 3.5 kDa was delivered by Spectrum Laboratories Inc., Breda, The Netherlands. Water was of MilliQ grade.

Polymer Characterization by Differential Scanning Calorimetry (DSC)

Thermoanalysis was performed on a Mettler Toledo DSC 821e scanning calorimeter to investigate glass transition temperatures and melting points of the polymers. All dry block copolymers were weighed into 100 µL aluminium pans. These samples were heated two times from −50°C to 100°C (PEG-PVPy samples to 200°C) with a heating and cooling rate of 10 K/min. After each heating or cooling ramp, an isothermal step of 5 min was implemented. The first heating and cooling cycle was used to clear thermal history of the polymers; the second heating cycle was used to evaluate thermal events. All experiments were performed in triplicate.

Micelle Preparation

Samples for Determination of Critical Aggregation Concentration (CAC)

For the determination of the CAC, the pyrene probing method described by Wilhelm *et al.* was used and further adapted to the requirements of the tested polymer types (21). This method is based on the change of vibrational fine structure of the fluorescence light emission spectra, which depends on the polarity of the probe environment (22).

Micelles were prepared by dissolving the polymers in acetone, reaching a final concentration of 0.5% *w/v*. This organic solution was directly dialyzed against 5 L water for 7 h. The water was changed twice. This preparation step forms dye-free micelles with very low residual solvent (data not shown).

In the second step, a pyrene stock solution was prepared and added to the dye-free polymeric micelles in a third step. The pyrene solution was prepared by dissolving the dye in tetrahydrofurane (THF, 6×10^{-2} mol/L). This solution was injected into water with a final pyrene concentration of 6×10^{-6} mol/L (stock solution). THF was removed by evaporation at 40°C and 50 mbar over 1 h.

As a third step, the dye-free polymeric micelles were diluted corresponding to a polymer concentration range from 1.0 mg/mL to 5×10^{-4} mg/mL. The samples were incubated over 12 h with the pyrene stock solution, enabling the partitition of pyrene into the micellar core. The pyrene concentration was kept constant in all samples at 1.2×10^{-7} mol/L.

Samples for Serum Incubation Studies, Asymmetrical Flow Field Flow Fractionation (AF4) Experiments, and Transmission Electron Microscopy (TEM)

DiI- and DiO-loaded polymeric micelles were prepared by solvent evaporation and finally a dialysis technique. Both dyes and the polymer were dissolved in acetone and added to water under stirring to reach a polymer target concentration of 2 mg/mL loaded with 0.0015% *w/v* of each dye. PEG-PVPy-based micelles were loaded with 0.0045% *w/v* donor (DiO) and 0.0015% *w/v* acceptor (DiI). The latter donor/acceptor (d/a) ratio was selected due to the light absorption properties of the vinylpyridine part in the block copolymer in contrast to the non-absorbing aliphatic polymers, such as PEG-PLLA, and is in line with investigations of Berney and Danuser (23). After evaporation overnight, the resulting micellar dispersion was filled into a dialysis bag and dialyzed over 4 h against 5 L water. This step was carried out to remove unentrapped fluorescence dye and residual solvent. Finally, the dispersion was filtered through a 0.2 µm celluloseacetate filter-membrane.

Micelle Characterization

Determination of Critical Aggregation Concentration (CAC)

Fluorescence excitation spectra of the pyrene-loaded micelles were recorded on an Aminco Bowman luminescence spectrometer (Aminco Bowman, Urbana, Illinois) at 390 nm emission wavelength and excitation wavelengths ranging from 300 nm to 360 nm using a spectral bandwidth of 1 nm and 2 nm for fluorescence excitation and emission, respectively. The scan rate was 0.5 nm/s. According to the

method of Wilhelm *et al.*, the $I_{338\ nm}/I_{334\ nm}$ ratio was evaluated for the determination of CAC (21). Each experiment was performed in triplicate.

Particle Size Measurements

The dynamic light scattering (DLS) technique was used to investigate the micellar average diameter. For the measurements, a Zetasizer Nano ZS90 from Malvern, UK, was set to 173° backscattering mode. The mean size and polydispersity index (PDI) were calculated by cumulants analysis using ZetasizerNano® software.

Transmission Electron Microscopy (TEM)

Micellar size and morphology were investigated by transmission electron microscopy using a negative staining technique. The samples were dried on the surface of carbon-coated copper grids (400 mesh; Plano, Wetzlar, Germany) for electron microscopy. For staining of PEG-PDLLA [5-b-23], a solution of 2% uranyl acetate solution in water (pH 4.5) was used, while all the other samples were stained using an aqueous solution of 2% phosphor tungistic acid (PTA; titrated to pH 7, using NaOH). The PEG-PLLA [5-b-4.7] sample was incubated with TritonX-100 for 20 min to examine the micellar destruction process as used in the FRET assay. All electron micrographs were digitally recorded using a CCD camera (TVIPS, Gauting) on a CM12 transmission electron microscope (FEI Electron Optics, Eindhoven, The Netherlands). For particle size determination, 100 particles in a predefined area of the electron micrograph were measured. Statistical evaluation was performed by calculation of arithmetic mean and standard deviation.

Determination of Micelles' *In Vitro* Serum Stability

Sample Incubation, FRET Ratio Determination, Calculation of Stability Parameters

Set-ups of fluorescence experiments were similar to the CAC determination. In contrast, excitation wavelength was set to 484 nm, and emission was scanned from 495 nm to 600 nm (for PEG-PVPy samples to 620 nm). All samples were incubated at 37°C over 3 h. Emission spectra were recorded after 0, 15, 30, 45, 60, 90, 120, and 180 min of incubation. Additionally, for PEG-PLGA [5-b-28] micelles, spectra at 4, 5, 6, 9, 12, 15, 18, and 26 h were recorded. After the last recording time point, micelles were dissolved by adding 7.5% *v/v* TritonX-100. The incubation was maintained for 20 min and a final spectrum was recorded.

Each single spectrum was integrated using Origin® software to determine the peak area of FRET-acceptor maximum and donor maximum. Calculating the FRET was done according to Eq. 1:

$$\text{FRET ratio} = \frac{\frac{\int_{D/A\,border}^{Spectrum\,end} intensity}{c[Acceptor]}}{\frac{\int_{Spectrum\,start}^{D/A\,border} intensity}{c[Donor]} + \frac{\int_{D/A\,border}^{Spectrum\,end} intensity}{c[Acceptor]}} \quad (1)$$

For each polymer, the interception point of the time-resolved fluorescence emission spectra was determined. By overlaying the recorded spectra, this interception point is defined before the emission peak of FRET acceptor dye (varying around 545 nm). "Spectrum start" was 495 nm emission wavelength for all DiO/DiI loaded micelles, whereas "spectrum end" was 600 nm apart from the PEG-PVPy micelles. For the latter, the spectra were integrated to 620 nm due to a wavelength shift caused by quenching effects of the dyes' fluorescent emission from pyridines' aromatic rings.

For quantitative evaluation of the data, the resulting FRET ratios were normalized to the TritonX-100 FRET ratio and the initial ratio at $t=0$ min by Eq. 2:

$$\text{Residual micellar fractions}[\%] = 100 \cdot \frac{FRET\ ratio_{t=x\,min} - FRET\ ratio_{TritonX-100}}{FRET\ ratio_{t=0\,min} - FRET\ ratio_{TritonX-100}} \quad (2)$$

Residual micellar fractions (RMFs) were plotted and analyzed by Origin® software using the first-order decay curve-fitting function. From the fitted curves at $RMF_{50\%}$, the serum half-life was calculated if possible. Additionally, the $RMF_{180\ min}$ was analyzed.

Asymmetrical Flow Field Flow Fractionation (AF4)

Due to the great versatility of AF4 concerning particle and protein separation (24), this method was selected to confirm the hypothesis of micellar disassembly in the presence of human serum. Therefore, dye-loaded PEG-PVPy [5-b-20] micelles, which showed intermediate stability in the described FRET assay, were incubated with human serum at 37°C. The incubation sample was prepared with a polymer concentration of 2 mg/mL and diluted with human serum (1:2). The samples were injected into a Wyatt Eclipse F module (Wyatt Inc., Santa Barbara, USA) with a 26.5 cm separation channel using a 350 µm polycarbonate spacer and polyethersulfone membrane with 5 kDa molecular weight cut-off (MWCO). The pump system consisted of an Agilent 1100 HPLC pump and degasser; detection was performed on a Wyatt DAWN EOS MALS detector and a Shodex RI-101 detector. A 50 mmol NaCl solution with 0.05% NaN_3 served as a mobile phase. The detector flow rate was 1.0 mL/min using a cross flow gradient from 3.0 mL/min to 0 mL/min, and the injection volume was 100 µL.

The original incubated sample was separated using AF4 0, 90, 180, 270, and 1,440 min after the beginning of incubation. During each separation run, the micellar fractions were collected (from 28 min to 33 min) and concentrated using Vivaspin 6 tubes. The resulting 5 mL sample volume from the first AF4 experiment was concentrated to 0.5 mL. Finally, this fraction was injected and separated again.

The presented size and size distribution equations were performed with Astra® 4 software. The particle diameters were calculated from RMS radii (d_{50}) in the particles mode, evaluating the angular dependence of scattered light assuming spherical particles. Based on the Zimm equation (25), the "90° MALS detector signal height" of the second separation step was used for semi-quantitative data evaluation of the concentrated samples.

RESULTS

Polymer and Micelles Characterization

The CAC of the tested block copolymers was studied due to its association with micellar thermodynamic stability. The CAC values of the polymeric micelles ranged from 0.41 to 5.71 mg/L (Fig. 1), which is considerably low compared to Tween 80® micelles (11.16 mg/L) and indicates a high stability upon dilution of block copolymer micelles. To validate the accuracy of the method used in this study, the CAC value for Tween 80® was compared with literature data which determined the CAC value by other methods. A good correlation was observed (e.g., surface tension measurement: 15.7 mg/L (26)).

Furthermore, from the CAC data of the different PEG-PVPy micelles, it was obvious that an increasing hydrophobic block length leads to a lower CAC, in agreement with published data (27). Comparing CAC values of micelles based on copolymers with similar hydrophobic to hydrophilic ratios, a decrease of CAC from PEG-PLGA to PEG-PVPy and PEG-PDLLA was observed.

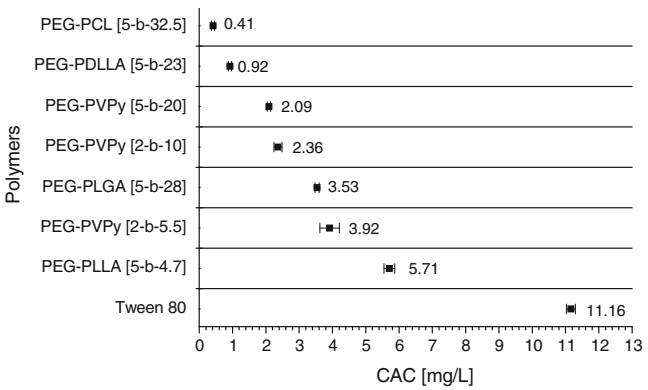

Fig. 1 CAC values of the investigated polymers determined by the pyrene method. Results are presented as mean ± SD ($n = 3$).

The architecture of the micellar core, which can be either crystalline or amorphous, plays an important role in the stability of polymeric micelles (27). Therefore, we investigated the thermal properties of the dry polymers as received (Table I). Differential scanning calorimetry revealed that PEG-PLLA [5-b-4.7] and PEG-PCL [5-b-32.5] showed crystalline characteristics with melting points above room temperature, whereas for the other investigated polymers glass transition temperatures that are typical for amorphous materials were detected in their thermograms. The glass transition temperatures of PEG-PDLLA [5-b-23] and PEG-PLGA [5-b-28] were below room temperature. In contrast, the investigated PEG-PVPy showed glass transition temperatures above 100°C. It is worth mentioning that the presence of water, encapsulated compounds, or residual solvents can act as plasticizers and greatly affect the nature of the hydrophobic core, changing it from crystalline to amorphous and/or reducing its glass transition temperature.

Micellar morphology and diameter were investigated by transmission electron microscopy (TEM) and dynamic light scattering (DLS). Results are summarized in Table II. DLS revealed that Tween 80® forms the smallest micelles with a hydrodynamic diameter of about 10 nm followed by the PEG-PVPy micelles ranging in size from ~28 nm to ~31 nm. The micelles of PEG-PLA derivatives, PEG-PLLA and PEG-PDLLA were ~49 nm and ~45 nm in diameter, respectively. PEG-PCL and PEG-PLGA form larger micelles with a diameter of around 80 nm. This trend in size can also be found in the TEM micrographs. They revealed nanosized particles of spherical shape independent of the copolymers used (Fig. 2). The mean particle diameter observed by TEM is either smaller than or equal to the hydrodynamic diameter measured by DLS.

Both PEG-PDLLA [5-b-23] and all PEG-PVPy-based micelles showed narrow and homogeneous particle size distribution in TEM micrographs, although the PDI in DLS was relatively high. On the other hand, a wider size distribution was obvious for PEG-PLGA [5-b-28]- and PEG-PCL [5-b-32.5]-based micelles in the TEM micrographs.

Taking the negative staining sample preparation technique into consideration, the single particles showed a bright grey micellar core surrounded by a shell-forming corona visible as dark shadows. This observation confirms the well-established core-shell model for polymeric micelles and had been shown also in TEM micrographs for drug-loaded micelles by Wang *et al.* (28).

The TEM micrographs of TritonX-100 and PEG-PLLA [5-b-4.7] were recorded to document the dissolution of the

Table I Physical State of Used Block Copolymers (Mean ± SD ($n = 3$))

Polymer type	Amorphous	Crystalline	T_g [°C]	T_m [°C]
PEG-PLLA [5-b-4.7]	–	X	–	46.23 ± 0.24
PEG-PDLLA [5-b-23]	X	–	5.07 ± 0.13	–
PEG-PLGA [5-b-28]	X	–	6.19 ± 0.57	–
PEG-PCL [5-b-32.5]	–	X	–	55.84 ± 1.05
PEG-PVPy [2-b-5.5]	X	–	101.83 ± 4.58	–
PEG-PVPy [2-b-10]	X	–	109.19 ± 2.54	–
PEG-PVPy [5-b-20]	X	–	136.36 ± 1.36	–

micelles by this detergent. The micrograph of TritonX-100 alone did not show any visible particles. Particle diameter obtained from DLS for TritonX-100 micelles are below 10 nm (data not shown). Incubation and preparation of PEG-PLLA and TritonX-100 show large particles in the micrograph without the typical core-shell structure. The contrasting agent was able to diffuse inside this larger particle and indicated the principle of micellar disintegration.

FRET Stability Assay

In this study, we used FRET as a direct marker of micellar integrity. Energy transfer from the fluorescence dyes DiO (emission maximum: 505 nm) to DiI (emission maximum: 575 nm) without light emission of DiO appears only when the distance between both molecules is in the lower nanometer range. Due to overlapping DiO emission and DiI excitation spectra, the DiI emission can be only observed after exciting DiO. This is the case in the micellar core.

Results and basic principle of this FRET assay are outlined in Fig. 3 for Tween 80® micelles. The final data evaluation process is presented in Fig. 4. All investigated polymeric micelles were analyzed accordingly, and the resulting data are summarized in Table III and Fig. 5.

The calculation of a half-life after incubation in human serum was possible for Tween 80®, PEG-PLGA, and all PEG-PVPy micelles, whereas for the other investigated polymers the calculated RMF values did not fall below 50%. All micellar disassemblies followed a first-order kinetic profile, with a good correlation observed ($R^2 > 0.90$). The PEG-PVPy micelles showed an increase in half-life with increasing molar masses of the hydrophobic part. The longest half-life which could be achieved with PEG-PVPy [5-b-20] was similar to Tween 80® micelles. In contrast PEG-PLGA formed more stable micelles and exhibited a half-life in this assay larger than 24 h. The more stable micelles are characterized by the RMF values above 50%. PEG-PCL, PEG-PDLLA, and PEG-PLLA micelles were the most stable ones investigated in this study. Moreover, the best stability in human serum was detected using PEG-PLLA-formed micelles showing nearly no influence of serum proteins on stability. Fig. 5 further illustrates that the investigated DiI/DiO-loaded polymeric micelles were stable upon dilution in water above CAC over a time period of 180 min at 37°C.

Asymmetrical Flow Field Flow Fractionation (AF4)

AF4 measurements were performed as a reference method to confirm micellar disassembly in the presence of human serum. Fig. 6 illustrates the results of the AF4 experiments. First, the behavior of the dye-loaded PEG-PVPy [5-b-20] micelles and human serum under the selected separation conditions was analyzed (Fig. 6a). The chromatogram of PEG-PVPy micelles showed a main peak ranging between 24 min to 31 min retention time. A sharp signal observed from the polymeric micelles indicated their high stability upon dilution in AF4 experiments. Although serum and

Table II Particle Sizes and Size Distributions of Polymeric Micelles Resulting from TEM and DLS (Mean ± SD)

Polymer	TEM size [nm]	DLS size [nm]	DLS PdI
Tween 80®	n.p.[a]	10.42 ± 0.03	0.091 ± 0.015
PEG-PLLA [5-b-4.7]	17.10 ± 6.10	49.34 ± 6.57	0.261 ± 0.010
PEG-PDLLA [5-b-23]	22.56 ± 4.07	45.07 ± 3.50	0.121 ± 0.031
PEG-PLGA [5-b-28]	32.09 ± 10.13	83.08 ± 3.86	0.136 ± 0.027
PEG-PCL [5-b-32.5]	37.77 ± 7.42	81.75 ± 4.74	0.060 ± 0.033
PEG-PVPy [2-b-5.5]	18.69 ± 3.51	29.77 ± 2.93	0.098 ± 0.047
PEG-PVPy [2-b-10]	23.59 ± 3.51	31.45 ± 1.66	0.183 ± 0.009
PEG-PVPy [5-b-20]	23.80 ± 4.51	28.28 ± 1.38	0.165 ± 0.011

[a] not possible with the used experimental setup: for a Cryo-TEM micrograph of Tween 80® micelles please refer to Sagalowicz *et al.* (29)

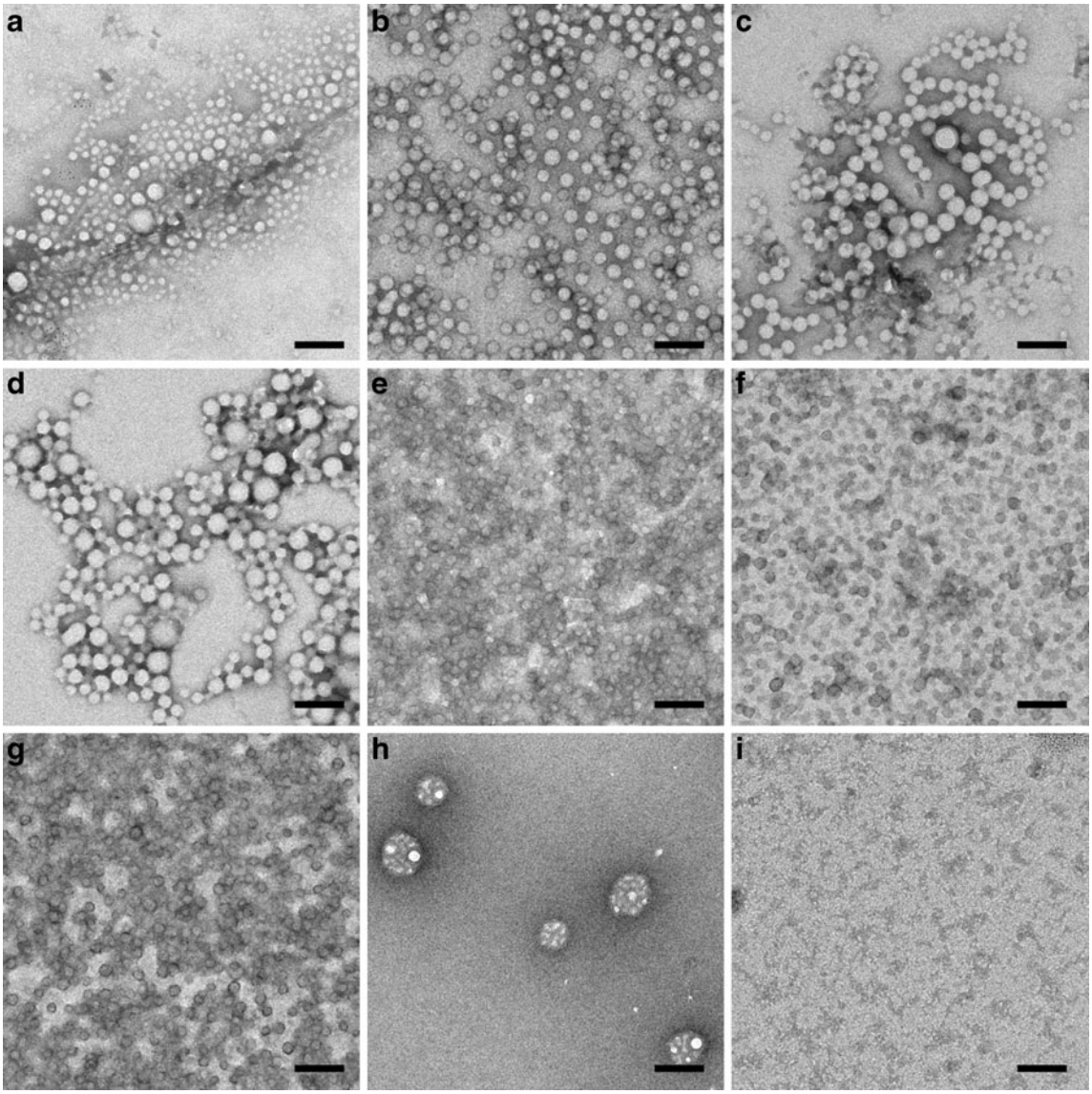

Fig. 2 TEM micrographs of block copolymer micelles, negatively stained using uranyl acetate (PEG-PDLLA) or phosphor tungstate (all other samples). Scale bar represents 100 nm. (**a**) PEG-PLLA [5-b-4.7]; (**b**) PEG-PDLLA [5-b-23]; (**c**) PEG-PLGA [5-b-28]; (**d**) PEG-PCL [5-b-32.5]; (**e**) PEG-PVPy [2-b-5.5]; (**f**) PEG-PVPy [2-b-10]; (**g**) PEG-PVPy [5-b-20]; (**h**) PEG-PLLA [5-b-4.7] incubated with TritonX-100 for 20 min at 37°C; (**i**) TritonX-100.

micellar signals are overlapping, Fig. 6a shows the detection of micelles in the presence of serum was possible due to slightly different hydrodynamic radii of serum proteins and micelles. Therefore, micelles and serum were mixed and investigated simultaneously in a second experiment (Fig. 6b). As shown in Fig. 6a by single micelles and serum fractograms, the micelles are detectable in the mixture at retention time between 28 min and 33 min. This fraction was collected and separated again to improve resolution. Finally, polymeric micelles were incubated in human serum at 37°C, and samples were analyzed at different time periods as described above (Fig. 6c). Table IV summarizes the changes in particle sizes of each process step.

Pure micelles showed particle diameters of ~22 nm, whereas immediately after addition of human serum the particle size increased to ~50 nm. During incubation, the particle diameters of the untreated sample increased continuously after 180 min incubation time to ~184 nm and declined to ~35 nm after 24 h. The particle size of the concentrated samples showed a different trend. During the second separation, the d_{50}-size parameter scatters around 22 nm ± 1.5 nm. This enabled the evaluation of the MALS detector peak height to correlate it with the particle concentration.

In Fig. 6d, 90° MALS detector signal height is shown for the concentrated samples over time. Its decrease followed a

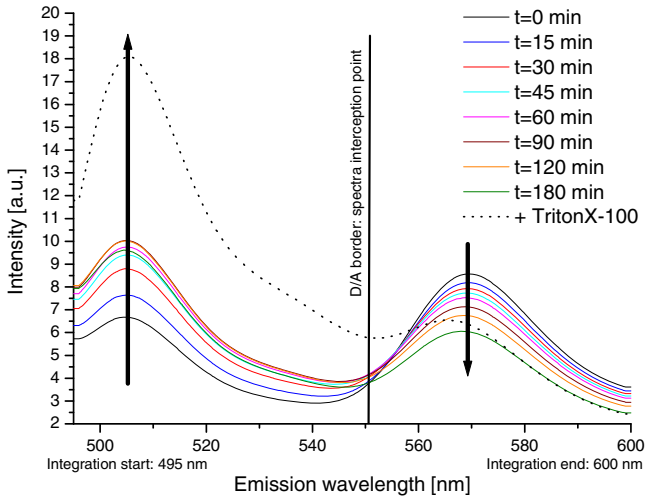

Fig. 3 Fluorescence spectra overlay for DiI/DiO-loaded Tween 80® micelles in human serum. The maximum at 570 nm emission wavelength originally comes from the acceptor DiI, the one at 505 nm from the donor DiO. The decreasing acceptor and increasing donor maximum indicate the micellar disassembly during sample incubation. After 3 h incubation time TritonX-100 was added. This destroys the micelles and leads to a complete dye release.

first-order kinetics, which was also observed in the FRET experiments.

DISCUSSION

In this study, different block copolymers were investigated for their applicability as a micellar drug delivery system. For its clinical development, it is of high interest to understand the fate of polymeric micelles after intravenous application (12). This issue is also highlighted by the regulatory authorities, as seen in the current guideline draft

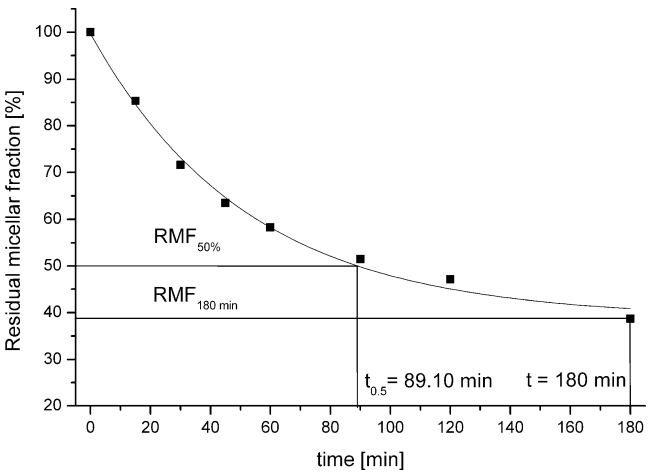

Fig. 4 RMF at different incubation times of Tween 80® micelles. Tween 80® micelles show a first-order disassembly kinetic. To compare varying block copolymers from the resulting graphs, the serum half-life ($t_{0.5}$) and the $RMF_{180\ min}$ were evaluated.

released by the EMA in the field of micellar formulations (30).

Block copolymers were composed of different chain lengths of polyethylene glycol as the hydrophilic part and varying hydrophobic parts with different molar masses. Physicochemical characterization revealed that all polymers were able to form nanosized micelles of spherical shape. The results show that particle size obtained from TEM often is much smaller compared to the results from DLS. One explanation for this observation could be the air-drying step involved in TEM sample preparation. The most probable reason is the different measurement principle of DLS and TEM. DLS delivers an intensity weighed size distribution of hydrodynamic radii based on the Rayleigh approximation (scattering intensity ~d^6), which finally overestimates the presence of larger micelles. Considering this factor, the large discrepancy between the results of both techniques is not unexpected.

The recorded TEM micrograph indicated that the addition of TritonX-100 to copolymer micelles led to a fusion of micelles. This goes along with FRET dye release obtained by fluorescence spectroscopy. The lysis of the nanoparticles was responsible for the decrease of the FRET ratio after TritonX-100 incubation. Similar disintegration effects of lipid membranes by detergent interaction have been described previously by Ahyayauch *et al.* (31).

Consequently, this enabled us to investigate the stability of different polymeric micelles in human serum. Dual-dye-loaded polymeric micelles were analyzed with a FRET-based technique. After fluorescence spectra integration and FRET ratio calculation, the two serum stability parameters residual micellar fractions (RMF) and serum half-lives were determined. Both parameters revealed highly relevant properties concerning stability.

In the FRET assay, PEG-PLLA [5-b-4.7], PEG-PDLLA [5-b-23], PEG-PLGA [5-b-28], and PEG-PCL [5-b-32.5] micelles exhibited an extended half-life longer than 24 h, whereas Tween 80® and PEG-PVPy micelles were more labile, with half-lives below 2 h. Fast disassembly of Tween 80® micelles was expected (FRET assay half-life ~1.5 h). This non-ionic surfactant was chosen as an ideal reference polymer to compare with the results from the block copolymers due to known very low *in vivo* stability. For instance, Lasseter *et al.* performed a tolerability and bioequivalency study of fosaprepitant compared to aprepitant, where the prodrug fosaprepitant was encapsulated in Tween 80® micelles and applied to healthy subjects (32). The pharmacokinetic data revealed that after injection the prodrug was completely metabolized to the active drug by ester hydrolysis in less than 45 min, indicating a full micellar destruction and drug release from the Tween 80® micelles. Thus, a comparison between Tween 80® and the block copolymer micelles in the developed *in vitro* assay was

Table III Stability of Different Block Copolymers in Human Serum. All Samples Follow First-Order Kinetics

Polymer	Quality of curve fitting (R^2)	$t_{0.5}$ [h]	$RMF_{180\ min}$ [%] (Mean ± SD)
Tween 80®	0.9924	1.48	38.73 ± 10.37
PEG-PLLA [5-b-4.7]	0.9886	≫26[a]	98.38 ± 1.00
PEG-PDLLA [5-b-23]	0.9901	≫26[a]	91.60 ± 1.28
PEG-PLGA [5-b-28]	0.9850	25.07	66.83 ± 1.23
PEG-PCL [5-b-32.5]	0.9946	≫26[a]	85.27 ± 1.24
PEG-PVPy [2-b-5.5]	0.9923	0.68	23.27 ± 10.37
PEG-PVPy [2-b-10]	0.9389	0.92	34.19 ± 2.57
PEG-PVPy [5-b-20]	0.9659	1.72	44.19 ± 4.26

[a] These micellar types exhibit very high serum stability in the assay; consequently, serum half-life was not calculated due to necessary extrapolation of the existing data

highly interesting and helps to better interpret the obtained stability parameters.

Comparing the stability based upon dilution values of the polymers with the serum values, it is obvious that micellar disassembly did not result from simple dilution phenomena as long as the final concentration is above the CAC. A major change in FRET ratio was not detectable after dilution of the samples in water still above CAC (Fig. 5).

However, in this study we furthermore investigated physicochemical properties of these micelle-forming block copolymers which are strongly linked with micellar stability: hydrophilic/hydrophobic ratio (33), particle sizes and particle size distributions (33), critical aggregation concentration (CAC) (27), and thermal status of the block copolymers (34,35).

Riley *et al.* reported for PEG-PLA micelles a dependence of serum stability on particle size and hydrophilic/hydrophobic ratio (33). While keeping a constant block length of the PEG part (5 kDa), an increase of hydrophobic block length led to larger micellar cores and finally larger particles. Consequently, the PEG shell had only a minor influence on the properties of micelles and can lead to incomplete coverage and protection of the core from environmental milieu (as postulated for PLA blocks larger than 30 kDa). According to Riley *et al.*, this partially leads to the presence of PLA carboxyl groups on the surface and confers the particles a surface charge, as indicated by zeta-potential measurements. Proteins could thus adsorb onto the less PEG-protected surface. Colloidal stability was investigated by addition of the nanoparticles to different amounts of Na_2SO_4 solution and the determination of the critical flocculation points (CFPT). Interestingly, copolymers with high molar mass PLA blocks (30 kDa and more) exhibited a lower CFPT before protein incubation and similar CFPTs after protein incubation compared to lower molar mass PLA blocks (<30 kDa). Riley *et al.*'s study revealed that incomplete PEG surface coverage did not lead to lower colloidal stability when designing micelles with larger PLA blocks (33). This postulated mechanism could be one explanation for the high stability of PEG-PDLLA [5-b-4.7] and PEG-PLLA [5-b-23] micelles, whereas thermodynamic and kinetic approaches could not fully explain the high stability of PLA-based micelles.

The FRET assay showed that PEG-PLLA [5-b-4.7] with a molar mass of around 10 kDa and a hydrophobic/hydrophilic ratio of nearly 1:1 exhibited much higher stability than PEG-PVPy [5-b-20] with a molar mass of 25 kDa and a ratio 1:5. The same result was found with

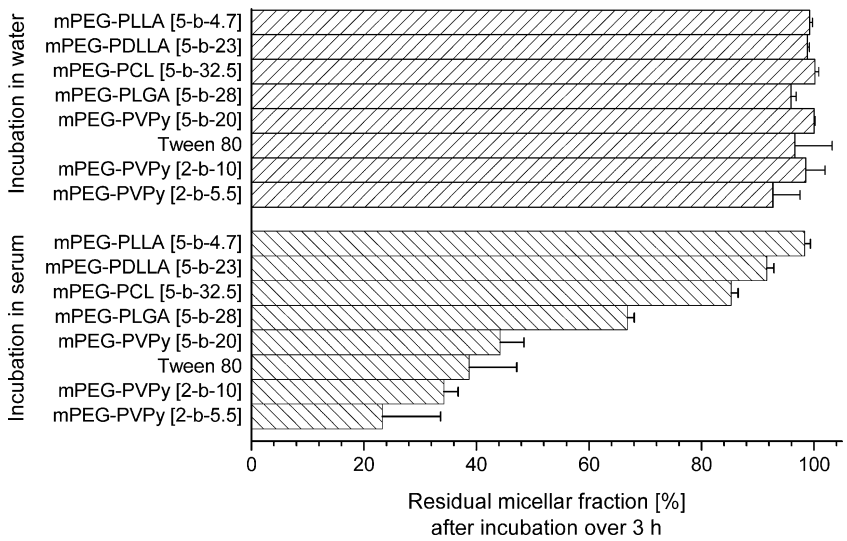

Fig. 5 Residual micellar fraction [%] of the investigated polymers determined by the FRET method in human serum compared to water. Results are presented as mean ± SD ($n = 3$).

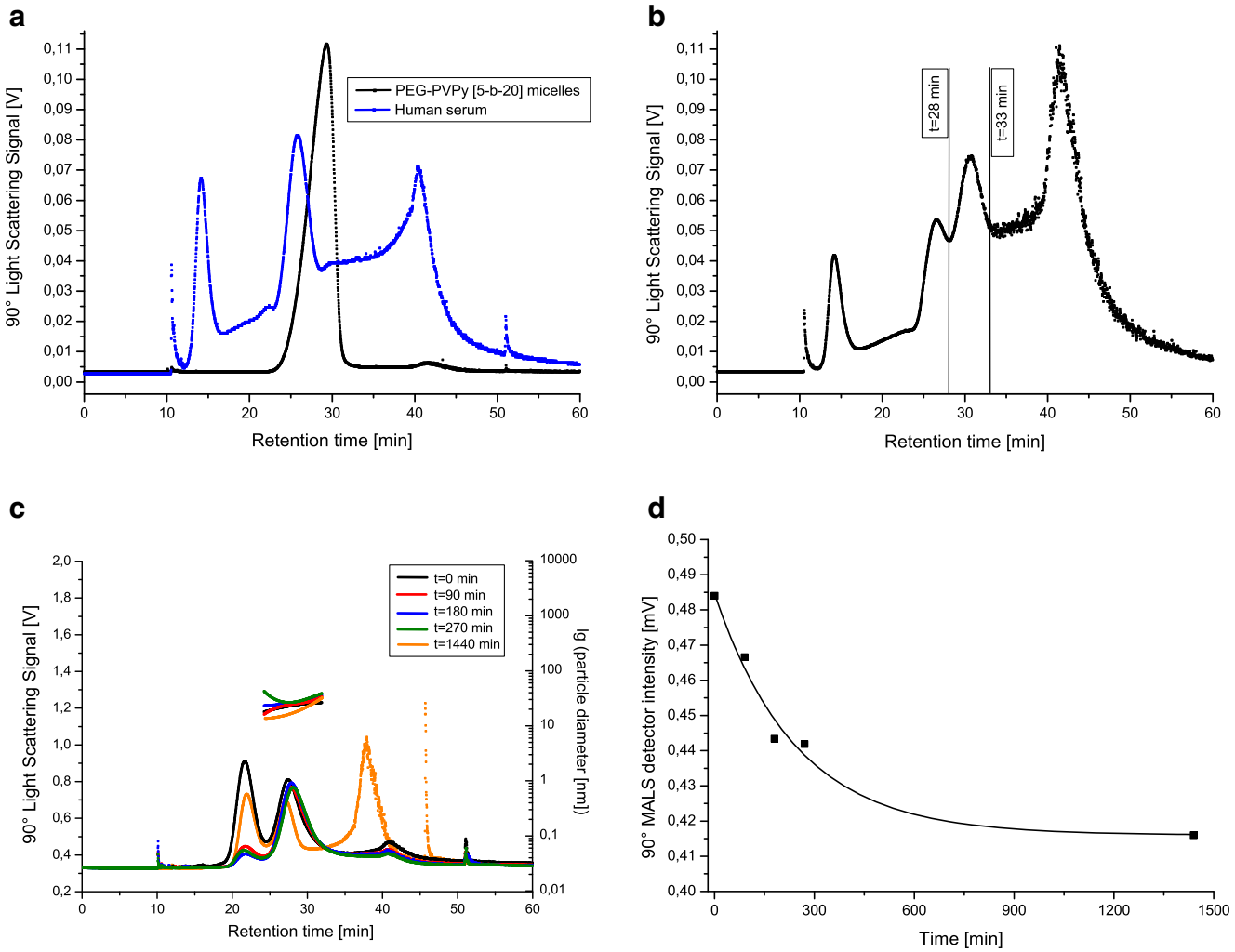

Fig. 6 Overlay of light scattering detector trace of dye-loaded micelles and human serum (**a**), dye-loaded micelles mixed with human serum (**b**), concentrated samples of dye-loaded micelles in human serum over time (**c**), intensity decay of light scattering detector signal height over sample incubation time, baseline corrected (**d**).

PEG-PLGA [5-b-28] (lower stability) and PEG-PLLA [5-b-23] (higher stability).

Consequently, the total molar masses and hydrophilic/hydrophobic ratios do not have a direct impact on micelle serum stability when comparing different block copolymers. In contrast, it was shown for the PEG-PVPy micelles with different PEG and vinylpyridine amounts in the molecule that an increasing hydrophobic part also increased the serum stability. Although PEG-PVPy [2-b-10] had a higher hydrophobic/hydrophilic ratio than PEG-PVPy [5-b-20], the latter was more stable, indicating that the size of the hydrophobic part is more decisive in determining the serum stability than the size of the PEG part. The same conclusion was drawn by Toncheva *et al.* when investigating the stability of PEG-polyorthoester ABA triblock polymers against bovine serum albumin (36).

Table IV PEG-PVPy [5-b-20] Micelles Diameter Determined by MALS Detector Signal After Incubation in Human Serum at Different Time Points

Sample status	Sample status	Particle diameter [d_{50} nm]
Micelles (pure)	Not processed	21.8
Micelles in presence of serum $t = 0$ min	Untreated	50.5
Micelles and serum $t = 90$ min	Untreated	182.9
Micelles and serum $t = 180$ min	Untreated	183.8
Micelles and serum $t = 270$ min	Untreated	166.1
Micelles and serum $t = 1{,}440$ min	Untreated	34.6

Thermodynamic stability of polymeric micelles is directly connected with the CAC. Data of CAC determination for the tested polymers showed that PEG-PCL (CAC~0.41 mg/L) micelles had the lowest aggregation onset, whereas PEG-PLLA (CAC~5.71 mg/L) micelles showed the highest CAC in this study. In contrast to the block copolymers, Tween 80®,

as a non-ionic surfactant, had an aggregation onset at a much higher concentration (~11.16 mg/L). Therefore, one would expect PEG-PCL micelles to be most stable, and PEG-PLLA micelles would be associated with lowest stability from a thermodynamic point of view.

The crystalline and/or amorphous nature of the dry polymer seems to have no connection with its *in vitro* serum stability. For instance, the thermograms of PEG-PLLA [5-b-4.7] (T_m~46°C) and PEG-PCL [5-b-32.5] (T_m~56°C) show melting events, while PEG-PLGA [5-b-28] (T_g~6°C), PEG-PDLLA [5-b-23] (T_g~5°C), and PEG-PVPy (T_g~102–136°C) are amorphous. If the hydrophobic core of the micelles was crystalline or frozen due to a high T_g, analogous to the dry polymer, then one would expect PEG-PVPy to be more stable than the "softer" polylactide copolymers, which was not the case in this study. The effect of micellar stabilities cannot be fully explained by the thermal properties, as is also shown by Jacquin *et al.* (34). This is because the presence of water or encapsulated material can act as plasticizer or crystallization inhibitor, thus changing the state of the hydrophobic micellar core compared to the dry polymer.

Finally, we aimed to clarify if the observed time-dependent changes in FRET effects are exclusively due to micellar disassembly in the presence of serum. There is still a possibility that the fluorescent dyes redistribute from the micellar core towards serum proteins. AF4 measurements were used to substantiate the FRET results and exclude the latter possibility.

For this experiment, PEG-PVPy [5-b-20] micelles were selected due to their intermediate stability in serum as determined by FRET measurements. The fact that during the elution of the pure micelles no peaks for the polymer appeared in the fractogram (before the micellar peak) shows that the micelles remained intact under the high dilution processes in the AF4 experiments.

While incubating the micelles with serum over time, we identified a method for semiquantitative data analysis involving the evaluation of signal height of light scattering. This light scattering intensity decreases over time in a first-order decay, showing similar kinetics to those found for the FRET experiments (Fig. 6d). It is highly probable that the effects seen in the FRET experiments were caused by micellar disassembly. Interestingly, the protein adsorption on the micellar shell can be followed via the particle diameter, which increased from the initial particle size of ~51 nm to 184 nm after 180 min incubation time and subsequently decreased down to ~35 nm after 24 h. FRET experiments confirmed that only minor changes in micellar concentrations can be expected after 120 min due to the observed first-order kinetics (Fig. 4). Saturation of micelles with serum proteins is highly probable. AF4 experiments further revealed that there are residual micelles with comparable size to freshly prepared ones still present after 24 h incubation time. Based on this observation, high adsorption of proteins on the micellar surface most likely occurred during the first few hours. However, when the stability influencing protein fraction is saturated with polymer monomers, the reaction rate slows down to a first-order kinetic. Additional data will be needed to confirm this hypothesis.

In summary, we could show that all investigated block copolymer micelles exhibited relatively high thermodynamical stability against dilution, whereas the serum stability differed extremely between the different polymers.

CONCLUSION

By using an improved FRET-based assay, we were able to discriminate between different block copolymers quantitatively in terms of *in vitro* serum stability. PEG-PVPy showed very low serum stability compared to the PEG-PLGA, PEG-PLA, and PEG-PCL. Within the same homologous series, the length of the hydrophobic chain was more decisive regarding the serum stability than the hydrophobic/hydrophilic ratio or the length of the PEG chain. Additionally, the crystalline/amorphous state of the hydrophobic chain in the dry polymer could not predict the serum stability of the polymeric micelles. AF4 experiments are one approach to confirm that a decrease in FRET ratio is due to micellar disassembly.

Although further relevance of our studies has to be carefully investigated in *in vivo* experiments, the presented techniques and results offer the possibility to screen novel polymers in terms of *in vitro* stability.

ACKNOWLEDGMENTS & DISCLOSURES

The authors thank Dr. Judith Kuntsche at the Martin Luther University Halle, Germany, for her help with the AF4 experiments. The support of Dr. Philip Hewitt and Alina Rwei, Merck KGaA Darmstadt, Germany, concerning language improvements is highly appreciated.

REFERENCES

1. Lipinski C. Poor aqueous solubility—an industry wide problem in drug discovery. Am Pharm Rev. 2002;5:82–5.
2. Adams ML, Lavasanifar A, Kwon GS. Amphiphilic block copolymers for drug delivery. J Pharm Sci. 2003;92:1343–55.
3. Jones M, Leroux J. Polymeric micelles—a new generation of colloidal drug carriers. Eur J Pharm Biopharm. 1999;48:101–11.
4. Kataoka K, Harada A, Nagasaki Y. Block copolymer micelles for drug delivery: design, characterization and biological significance. Adv Drug Deliv Rev. 2001;47:113–31.

5. Aliabadi HM, Shahin M, Brocks DR, Lavasanifar A. Disposition of drugs in block copolymer micelle delivery systems: from discovery to recovery. Clin Pharmacokinet. 2008;47:619–34.
6. Greish K. Enhanced permeability and retention (EPR) effect for anticancer nanomedicine drug targeting. Methods Mol Biol. 2010;624:25–37.
7. Wiradharma N, Zhang Y, Venkataraman S, Hedrick JL, Yang YY. Self-assembled polymer nanostructures for delivery of anticancer therapeutics. Nano Today. 2009;4:302–17.
8. Wang J, Sui M, Fan W. Nanoparticles for tumor targeted therapies and their pharmacokinetics. Curr Drug Metab. 2010;11:129–41.
9. Hamaguchi T. Cancer chemotherapy utilizing nanotechnology. Gan To Kagaku Ryoho. 2009;36:372–6.
10. Kim SC, Kim DW, Shim YH, Bang JS, Oh HS, Wan KS, *et al. In vivo* evaluation of polymeric micellar paclitaxel formulation: toxicity and efficacy. J Control Release. 2001;72:191–202.
11. Chung TW, Liu DZ, Hsieh JH, Fan XC, Yang JD, Chen JH. Characterizing poly(epsilon-caprolactone)-b-chitooligosaccharide-b-poly(ethylene glycol) (PCP) copolymer micelles for doxorubicin (DOX) delivery: effects of crosslinked of amine groups. J Nanosci Nanotechnol. 2006;6:2902–11.
12. Kim S, Shi Y, Kim JY, Park K, Cheng JX. Overcoming the barriers in micellar drug delivery: loading efficiency, *in vivo* stability, and micelle–cell interaction. Expert Opin Drug Deliv. 2010;7:49–62.
13. Gaucher G, Marchessault RH, Leroux JC. Polyester-based micelles and nanoparticles for the parenteral delivery of taxanes. J Control Release. 2010;143:2–12.
14. Chen H, Kim S, He W, Wang H, Low PS, Park K, *et al.* Fast release of lipophilic agents from circulating PEG-PDLLA micelles revealed by *in vivo* forster resonance energy transfer imaging. Langmuir. 2008;24:5213–7.
15. Chen H, Kim S, Li L, Wang S, Park K, Cheng JX. Release of hydrophobic molecules from polymer micelles into cell membranes revealed by Forster resonance energy transfer imaging. Proc Natl Acad Sci USA. 2008;105:6596–601.
16. Kamat PV, Fox MA. Photophysics and photochemistry of xanthene dyes in polymer-solutions and films. J Phys Chem. 1984;88:2297–302.
17. Cerritelli S, Velluto D, Hubbell JA, Fontana A. Breakdown kinetics of aggregates from poly(ethylene glycol-bl-propylene sulfide) di- and triblock copolymers induced by a non-ionic surfactant. J Polym Sci A Polym Chem. 2008;46:2477–87.
18. Gref R, Luck M, Quellec P, Marchand M, Dellacherie E, Harnisch S, *et al.* 'Stealth' corona-core nanoparticles surface modified by polyethylene glycol (PEG): influences of the corona (PEG chain length and surface density) and of the core composition on phagocytic uptake and plasma protein adsorption. Colloids Surf B Biointerf. 2000;18:301–13.
19. Aliabadi HM, Brocks DR, Mahdipoor P, Lavasanifar A. A novel use of an *in vitro* method to predict the *in vivo* stability of block copolymer based nano-containers. J Control Release. 2007;122:63–70.
20. Savic R, Luo L, Eisenberg A, Maysinger D. Micellar nanocontainers distribute to defined cytoplasmic organelles. Science. 2003;300:615–8.
21. Wilhelm M, Zhao CL, Wang YC, Xu RL, Winnik MA, Mura JL, *et al.* Poly(styrene-ethylene oxide) block copolymer micelle formation in water—a fluorescence probe study. Macromolecules. 1991;24:1033–40.
22. Kalyanasundaram K, Thomas JK. Environmental effects on vibronic band intensities in pyrene monomer fluorescence and their application in studies of micellar systems. J Am Chem Soc. 1977;99:2039–44.
23. Berney C, Danuser G. FRET or no FRET: a quantitative comparison. Biophys J. 2003;84:3992–4010.
24. Fraunhofer W, Winter G. The use of asymmetrical flow field-flow fractionation in pharmaceutics and biopharmaceutics. Eur J Pharm Biopharm. 2004;58:369–83.
25. Zimm BH. The scattering of light and the radial distribution function of high polymer solutions. J Chem Phys. 1948;16:1093–9.
26. Zheng Z, Obbard JP. Evaluation of an elevated non-ionic surfactant critical micelle concentration in a soil/aqueous system. Water Res. 2002;36:2667–72.
27. Allen C, Maysinger D, Eisenberg A. Nano-engineering block copolymer aggregates for drug delivery. Colloids Surf B-Biointerf. 1999;16:3–27.
28. Wang L, Zeng R, Li C, Qiao R. Self-assembled polypeptide-block-poly(vinylpyrrolidone) as prospective drug-delivery systems. Colloids Surf B Biointerf. 2009;74:284–92.
29. Sagalowicz L, Leser ME, Watzke HJ, Michel M. Monoglyceride self-assembly structures as delivery vehicles. Trends Food Sci Technol. 2006;17:204–14.
30. European Medicines Agency. Reflection paper on the pharmaceutical development of intravenous medicinal products containing active substances solubilised in micellar systems (non-polymeric surfactants). EMA/CHMP/QWP/574767/2010 (2010).
31. Ahyayauch H, Bennouna M, Alonso A, Goni FM. Detergent effects on membranes at subsolubilizing concentrations: transmembrane lipid motion, bilayer permeabilization, and vesicle lysis/reassembly are independent phenomena. Langmuir. 2010;26:7307–13.
32. Lasseter KC, Gambale J, Jin B, Bergman A, Constanzer M, Dru J, *et al.* Tolerability of fosaprepitant and bioequivalency to aprepitant in healthy subjects. J Clin Pharmacol. 2007;47:834–40.
33. Riley T, Govender T, Stolnik S, Xiong CD, Garnett MC, Illum L, *et al.* Colloidal stability and drug incorporation aspects of micellar-like PLA-PEG nanoparticles. Colloids Surf B-Biointerf. 1999;16:147–59.
34. Jacquin M, Muller P, Cottet H, Theodoly O. Self-assembly of charged amphiphilic diblock copolymers with insoluble blocks of decreasing hydrophobicity: from kinetically frozen colloids to macrosurfactants. Langmuir. 2010;26:18681–93.
35. Theodoly O, Jacquin M, Muller P, Chhun S. Adsorption kinetics of amphiphilic diblock copolymers: from kinetically frozen colloids to macrosurfactants. Langmuir. 2009;25:781–93.
36. Toncheva V, Schacht E, Ng SY, Barr J, Heller J. Use of block copolymers of poly(ortho esters) and poly (ethylene glycol) micellar carriers as potential tumour targeting systems. J Drug Target. 2003;11:345–53.